Cellular & Molecular Immunology (2014) 11, 467–476

www.nature.com/cmi

RESEARCH ARTICLE

Ly49 receptors activate angiogenic mouse DBA$^+$ uterine natural killer cells

Patricia DA Lima[1,2], Megan M Tu[1], Mir Munir A Rahim[1], Annie R Peng[1,2], B Anne Croy[2] and Andrew P Makrigiannis[1]

In humans, specific patterns of killer immunoglobulin-like receptors (KIRs) expressed by uterine natural killer (uNK) cells are linked through HLA-C with pregnancy complications (infertility, recurrent spontaneous abortion, intrauterine growth restriction and preeclampsia). To identify mechanisms underpinning the associations between NK cell activation and pregnancy success, pregnancies were studied in mice with genetic knockdown (KD) of the MHC-activated Ly49 receptor gene family. B6.Ly49^{KD} pregnancies were compared to normal control B6.Ly49^{129} and C57BL/6 (B6) pregnancies. At mid-pregnancy (gestation day (gd9.5)), overall uNK cell (TCRβ$^-$CD122$^+$DBA$^+$DX5$^-$ (DBA$^+$DX5$^-$)) and TCRβ$^-$CD122$^+$DBA$^-$DX5$^+$ (DBA$^-$DX5$^+$)) frequencies in pregnant uterus were similar between genotypes. Ly49^{KD} lowered the normal frequencies of Ly49$^+$ uNK cells from 90.3% to 47.8% in DBA$^-$DX5$^+$ and 78.8% to 6.3% in DBA$^+$DX5$^-$ uNK cell subtypes. B6.Ly49^{KD} matings frequently resulted in expanded blastocysts that did not implant (subfertility). B6.Ly49^{KD} mice that established pregnancy had gestational lengths and litter sizes similar to controls. B6.Ly49^{KD} neonates, however, were heavier than controls. B6.Ly49^{KD} implantation sites lagged in early (gd6.5) decidual angiogenesis and were deficient in mid-pregnancy (gd10.5) spiral arterial remodelling. Ultrastructural analyses revealed that B6.Ly49^{KD} uNK cells had impaired granulogenesis, while immunocytochemistry revealed deficient vascular endothelial cell growth factor (VEGFA) production. Perforin and IFNG expression were normal in B6.Ly49^{KD} uNK cells. Thus, in normal mouse pregnancies, Ly49 receptor signaling must promote implantation, early decidual angiogenesis and mid-pregnancy vascular remodelling. Disturbances in these functions may underlie the reported genetic associations between human pregnancy complications and the inability of specific conceptus MHCs to engage activating KIR on uNK cells.

Cellular & Molecular Immunology (2014) **11,** 467–476; doi:10.1038/cmi.2014.44; published online 23 June 2014

Keywords: fetal growth deviation; granule biogenesis; MHC-I receptors; uterine natural killer cells; vascular endothelial cell growth factor

INTRODUCTION

Natural killer (NK) cells are recruited in abundance to decidualizing endometrium early in pregnancy.[1–3] In humans, activation of uterine NK (uNK) cells has been genetically linked with fertility. In contrast, human infertility and gestational complications such as recurrent spontaneous abortion, intrauterine growth restriction and preeclampsia, are seen in specific maternal killer immunoglobulin-like receptors (KIRs) and fetal HLA-C gene combinations that evoke NK cell inhibitory signals.[4–8] Mechanisms explaining the roles of KIR in human fertility promotion are only beginning to be identified.[9] In normal human pregnancies, functions of uNK cells include angiogenesis, initiation of spiral artery modification and promotion of trophoblast invasion.[9–12]

Mouse uNK cells are largely analogous to those in humans and interact with H-2 *via* Ly49 molecules, a lectin receptor family with inhibitory and activing members. Mouse uNK cells promote uterine lumen closure, angiogenesis, the rate of early fetal development and they initiate spiral artery remodelling.[13–15] In contrast to human uNK cells, mouse uNK cells appear in the uterus after implantation rather than following the menstrual cycle surge luteinizing hormone.[16,17] Although mouse trophoblast cells express MHC molecules,[18] mouse uNK cells may have only an indirect influence on trophoblast invasion.[14]

[1]Department of Biochemistry, Microbiology and Immunology, University of Ottawa, Ottawa, ON K1N 6N5, Canada and [2]Biomedical and Molecular Sciences, Queen's University, Kingston, ON K7L 3N6, Canada
Correspondence: Dr PDA Lima, Ottawa Hospital Research Institute, The Ottawa Hospital General Campus, Critical Care Wing, 3rd Floor, Room W3129, 501 Smyth Road, Ottawa, ON CA K1H 8L6, Canada
E-mail: plima@ohri.ca
Received: 2 May 2014; Accepted: 14 May 2014

UNK cells in both humans and mice synthesize cytoplasmic granules that contain perforin and granzymes;[19–21] however, uNK cells are generally regarded as displaying limited lytic activity. Mouse, but not human, uNK cells bind *Dolichos biflorus* agglutinin (DBA) lectin[17,22] to membranes of the cell and of their numerous cytoplasmic granules. DBA lectin distinguishes two uNK cell subsets that can be separated as, DBA^+ and DBA^- by flow cytometry.[23,24] In early mouse pregnancy (gestational day (gd) 6.5), DBA^+ and DBA^- uNK cells are equivalent in frequency.[23] Then, the DBA^+ uNK cell subset becomes rapidly dominant.[16,21,23,24] Cytometric analyses of gd9.5 B6 decidua identified DBA^- uNK cells as $DX5^+NKp46^+NKG2D^+$ and the subset producing IFNG.[23,24] DBA^+ uNK cells were phenotyped as $DX5^-NKp46^+NKG2D^+$. The latter subset has more abundant expression of vascular endothelial growth factor (*Vegf*) and placental growth factor (*Pgf*),[24] important angiokines. DBA^+ uNK cells additionally express delta-like ligand-1, a NOTCH signaling protein critical for endothelial tip cell induction, perpendicular arterial branching and perivascular cell maturation.[25–27] These data suggested that DBA^+ uNK cells are a specialize, decidua-associated angiogenic subset. uNK cells express Ly49 receptors[23] but no information exists on whether DBA^+ or DBA^- uNK cell differentiation or functions depend on Ly49 receptor engagement or whether Ly49 receptor signaling impacts upon fecundity.

Ly49 receptors are highly polymorphic, type II transmembrane glycoproteins. They are encoded by multiple allelic genes in the NK gene complex (NKC) found on mouse chromosome 6.[28] Ly49 gene clusters differ between inbred mice strains (C56BL/6, 129/J, BALB/c, and NOD mice). In B6, the Ly49 gene cluster encodes two activating receptors (Ly49D, H), eight inhibitory receptors (Ly49Q, E, F, I, G, J, C, A) and five pseudogenes. In contrast, the 129-Ly49 gene cluster encodes three activating receptors (Ly49R, U, P), nine inhibitory receptors ($Ly49Q_1$, E, V, EC_2, S, T, I_1, G, O) and seven pseudogenes.[29] Mice with broad-spectrum KD (knockdown) of Ly49 expression ($B6.Ly49^{KD}$, also referred to as NKC^{KD}), were created and characterized by our group.[30] Approximately 80% of Ly49 receptor expression is reduced in NK cells in the spleens of these mice due to a concatemer insertion of the gene-targeting vector in the Ly49 region of the NKC. As a result, the ability of $B6.Ly49^{KD}$ NK cells to reject class I MHC-deficient cells is greatly impaired.[30] To address our hypothesis that engagement of Ly49 receptors by ligands endogenous to the maternal/fetal interface contributes to uNK cell activation and function within implantation sites we investigated pregnancies in $B6.Ly49^{KD}$ mice. We identified roles for Ly49 receptors beyond those reported for human KIR, specifically in uNK cell granule biogenesis and in enhancement of decidual vascular endothelial cell growth factor (VEGFA) production.

MATERIALS AND METHODS

Animals

C57BL/6 (B6), $B6.Ly49^{KD}$ and $B6.Ly49^{129}$ congenic ($B6.Ly49^{129}$) mice were used. B6 mice were purchased from The Jackson Laboratory (Bar Harbor, ME, USA). $B6.Ly49^{KD}$ (also known as NKC^{KD} and $Klra15^{tm1.1Apma}$) and $B6.Ly49^{129}$ congenic mice possessing the 129S1 Ly49 gene cluster on the B6 background[30,31] were bred at University of Ottawa as controls. All mice were maintained in a specific pathogen-free environment. Syngeneic matings were performed using mice over 6 weeks of age; copulation plugs were considered gd0.5; euthanasia was by cervical dislocation. All breeding and animal manipulations were conducted in accordance with guidelines of the Canadian Council on Animal Care and under animal utilization protocols approved by the University of Ottawa Animal Care Committee.

Flow cytometry

Females at gd9.5 (n=5/genotype) were euthanized and the implantation sites were collected. The mural mesometrial lymphoid aggregate of pregnancy (MLAp) and the decidua basalis were both dissected, placed together in RPMI 1640 medium (HyClone; Thermo Scientific, Inc. Waltham, MA, USA) on ice, pressed through a 70 μm cell strainer and washed with phosphate-buffered saline (PBS). Lymphocytes were enriched from 2×10^7 cells by gradient centrifugation on Lympholyte M (Cedarlane, Burlington, ON, CA) following the manufacturer's recommendations, washed in phosphate-buffered saline (PBS) and viable cells were counted. Equal numbers of cells were aliquoted, blocked with anti-CD16/CD32 (2.4G2) (BD Biosciences, Mississauga, ON, CA) and stained with antibodies (Table 1) for flow cytometric analysis as previously described.[30] Dead cells were excluded using propidium iodide (BD Biosciences). The frequencies of DBA^+DX5^- and DBA^-DX5^+ uNK cells were quantified amongst total $TCR\beta^-CD122^+$ decidual leukocytes. Ly49 receptor expression was analysed on $TCR\beta^-CD122^+DBA^+DX5^-$ and $TCR\beta^-CD122^+DBA^-DX5^+$ uNK cell subsets. Data were acquired using a CyAN-ADP flow cytometer (Beckman Coulter) and analysed with Kaluza software (BD Biosciences, Mississauga, ON, CA).

Morphological analyses

Ultrastructure. One cubic millimetre pieces of gd8.5, 9.5 and 10.5 decidua basalis (n=2 pregnancies with multiple implant sites used from each genotype and gestational day) were fixed in 2% paraformaldehyde, 2.5% glutaraldehyde in 0.1 M phosphate buffer and 0.1 M sucrose for 24 h, followed by post-fixation in 1% osmium tetroxide for 1 h at room temperature (RT). Standard procedures for dehydration and Epon resin embedding (Electron Microscopy Science) were performed following manufacturer's recommendations. Semi-thin and ultra-thin sections were contrasted with uranyl acetate and lead citrate, and micrographs were taken on a Hitachi 7000 transmission electron microscope.

Histological analyses. Implantation sites from gd9.5 and 10.5 (n=3 females with multiple implant sites used from each genotype and gestational day) and testis (n=2 males/genotype) were fixed by immersion in 4% paraformaldehyde for 24 h followed by processing into paraffin blocks. Six μm sections were stained with H&E or used for lectin cytochemistry[22] or immunohistochemistry, with or without antigen retrieval by Tris-EDTA (10 mM) pH 9.0, or citrate buffer (10 mM) pH 6.0 at 95 °C

Table 1 Information and reagents list used

Primary antibody	*Company*	*Method*	*Secondary antibody*	*Company*	*Method*
e780 anti-mouse TCRβ	eBioscience	Flow cytometry	Alexa-fluor 594 anti-rabbit	Invitrogen	Immunochemistry
PE anti-mouse CD122	eBioscience	Flow cytometry	Alexa-fluor 594 anti- rat	Invitrogen	Immunochemistry
APC anti-mouse DX5	BioLegend	Flow cytometry	*Isotype controls*	*Company*	*Method*
FITC 4D11	eBioscience	Flow cytometry	FITC mouse IgG2a	eBioscience	Flow cytometry
FITC 14B11	eBioscience	Flow cytometry	FITC golden Syrian	eBioscience	Flow cytometry
FITC 4E5	BioLegend	Flow cytometry	PE rat IgG2a,k	eBioscience	Whole-mount
Alexa-fluor 488 anti-mouse actin	eBioscience	Immunochemistry	Alexa-fluor 488 mouse IgG1, kappa	e-Bioscience	Immunochemistry
Rabbit anti-mouse VEGFA	Abcam	Immunochemistry: Tris-EDTA, pH 9.0	*Lectins and streptoavidins*	*Company*	*Method*
Rat anti-mouse perforin	Abcam	Immunochemistry: Tris-EDTA, pH 9.0	FITC and Texas-red DBA lectin	Sigma	Cytochemistry
Rabbit anti-bovine cytokeratin	Dako	Immunochemistry: citrate buffer, pH 6.0	Biotin DBA lectin	Sigma	Flow cytometry/Cytochemistry
PE anti-mouse CD31	BD Pharmigen	Whole-mount	e450-Streptoavidin	eBioscience	Flow cytometry

Abbreviations: DBA, *Dolichos biflorus* agglutinin; VEGFA, vascular endothelial cell growth factor.
List of antibodies, lectins and streptavidins used for flow cytometry, immunocytochemistry, cytochemistry and whole-mount *in situ* immunohistochemistry.

for 15 min. Reagents used for staining are listed in Table 1. For immunofluorescence, nuclei were visualized using ProLong Gold anti-fade reagent containing DAPI (Invitrogen, Life Technology, Burlington, ON, CA). Sections were examined and photographed using bright field or epifluorescence microscopy (Axiovision software; Zeiss Axiocam, Toronto, ON, Canada).

Morphometry. Spiral artery measurements were performed using 12 H&E stained sections from each gd10.5 implantation site (n=3 females with two or more implant sites studied per genotype; minimum 72 scored sections). Photomicrographs were acquired, maximum spiral artery wall and lumen diameters were measured on vessels cut in cross section and wall/lumen diameter ratios were calculated. All measurements were conducted blind to sample genotype.

Whole-mount immunohistochemistry. Gd6.5 uterine horns (n=2 pregnancies/genotype) were transected and stained with reagents listed in Table 1 as live, intact tissue as previously described.[32] Specimens were examined and photographed after 60 min using epifluorescence microscopy (Axiovision computer software; Zeiss Axiocam).

IFNG quantification

The mesometrial region (combined MLAp and decidua basalis) was dissected from implantation sites of gd10.5 females (n=4/genotype). These were pooled by litter, homogenized and lysed using a buffer containing protease inhibitors (1% Nonidet P-40 in 50 mM Tris–HCl, 5 mM EDTA buffer, supplemented with 2 mM phenylmethanesulfonyl fluoride and complete protease inhibitor cocktail (Roche Applied Science, Indianopolis, IN, USA)), and then centrifuged (17000*g*, 30 min, 4 °C). Supernatants were collected and stored at −80 °C until experimental use. Protein was quantified using Bradford reagent (Bio-Rad Laboratories, Mississauga, ON, CA). IFNG expression was measured by a FlowCytomix bead-based assay (eBioscience, San Diego, CA, USA), following manufacturer's instructions.

Fecundity

Five years of breeding records related to litter size and sex were analysed to compare fecundity between genotypes (n>20/genotype). Pup weights (n=4 litters totaling 25–34 pups/genotype) were recorded each morning from birth to post-partum day 7. To determine the exact length of pregnancy, gestation length was measured for five females/genotype between vaginal plug detection and delivery. Intrapartum litter sizes and viability were scored visually following euthanasia of pregnant females (n=~100/genotype). Timing of pre-implantation development was assessed by uterine flushing at gd3.5 (n=3/genotype).[33]

Statistical analyses

One-way ANOVA followed by Bonferroni's post-test was used to compare total numbers of DBA^+DX5^- and DBA^-DX5^+ uNK cells, IFNG levels, wall/lumen ratios of spiral arteries and pup birth weights. Analyses of sterile mating outcomes (absence of pregnancy following detection of a copulation plug) was performed by considering the mated, non-pregnant state as 0 and the mated, pregnant state as 1 (n>50) using Student's t-test. t-test was also used as an additional test to evaluate IFNG levels. Litter size comparisons were performed by two-way ANOVA. For all analyses, significance was considered at $P \leqslant 0.05$. Analyses employed GraphPad Prism V software (GraphPad Software, La Jolla, CA, USA).

RESULTS

KD of Ly49 expression does not alter uNK numbers

At gd9.5, $TCR\beta^-CD122^+$ decidual leukocytes were characterized as approximately 45% DBA^+DX5^- and 20% DBA^-DX5^+ uNK cells in the three genotypes (B6, B6.Ly49^{129} and

B6.Ly49^{KD}) (P>0.05; Figure 1). The lower frequency of DBA$^+$DX5$^-$ uNK cells in B6.Ly49^{KD} mice did not reach statistical significance (Figure 1b). Thus, the Ly49-deficiency of B6.Ly49^{KD} mice did not alter the recruitment of uNK cells to decidua and did not significantly deviate the DBA$^+$ *versus* DBA$^-$uNK cell subset distribution.

To address Ly49 expression by uNK cells, flow cytometric analysis of gd9.5 decidual leukocytes was undertaken. The majority of DBA$^+$DX5$^-$ (uterine unique) and DBA$^-$DX5$^+$ (peripheral blood-like) uNK cells expressed Ly49 receptors in the congenic strain (78.8% DBA$^+$DX5$^-$ and 90.3% DBA$^-$DX5$^+$ uNK cells; Figure 1a). This level of expression was comparable to that observed and previously reported for B6 uNK cells.[23] In B6.Ly49^{KD} mice, the number of DBA$^+$DX5$^-$ uNK cells expressing Ly49 was reduced by 92%, while the number of DBA$^-$DX5$^+$ uNK cells expressing Ly49 was reduced by 48.2% (Figure 1a). Thus, *Ly49* gene KD reduced receptor expression by DBA$^+$DX5$^-$ and by DBA$^-$DX5$^+$ uNK cells, but had an apparently larger effect on the angiogenic DBA$^+$ DX5$^-$ uNK cell subset.

Ultrastructural impact of Ly49 KD on uNK cells

To address the effects of loss of Ly49 on uNK cells, ultrastructural studies were undertaken between gd8.5 and 10.5. Most gd8.5 uNK cells are agranular,[17] while most gd10.5 uNK cells contain cytoplasmic granulates. Non-granulated uNK cells are more common in the MLAp, while granulated uNK cells are prevalent in decidua basalis and granule number is widely held to reflect uNK cell maturation. In uNK cells lacking cytoplasmic granules, no differences were seen between B6.Ly49^{KD} mice and controls (data not shown). In contrast, in uNK cells with cytoplasmic granules, Ly49 KD impaired granulogenesis. Cytoplasmic granules of control uNK cells had the two typically reported, morphologically distinct compartments of secretory-lysosomal granules (Figure 2ai). Cytoplasmic granules in B6.Ly49^{KD} uNK cells were mixtures of typical and abnormal granules with abnormal granule predominance. The abnormal granules were smaller, irregularly-shaped (Figure 2aii and iii) and often had only a single compartment (Figures 2aii). Additionally, a much higher frequency of multivesicular bodies occurred in B6.Ly49^{KD} than in control uNK cell cytoplasm, suggesting failure of granule biogenesis (Figure 2aiv).

Impact of Ly49 KD on VEGFA, perforin and IFNG

VEGFA is secreted through cytoplasmic vesicles in both agranular and granulated DBA$^+$DX5$^-$ uNK cells.[21] In gd10.5 B6.Ly49^{KD} uNK cells from MLAp or decidua basalis, VEGFA immunoreactivity was greatly decreased in intensity and frequency of expressing cells compared to either control strain (Figure 2b).

While VEGFA is localized into cytoplasmic vesicles, perforin occurs in the secretory-lysosomal granules of uNK cells. Not all

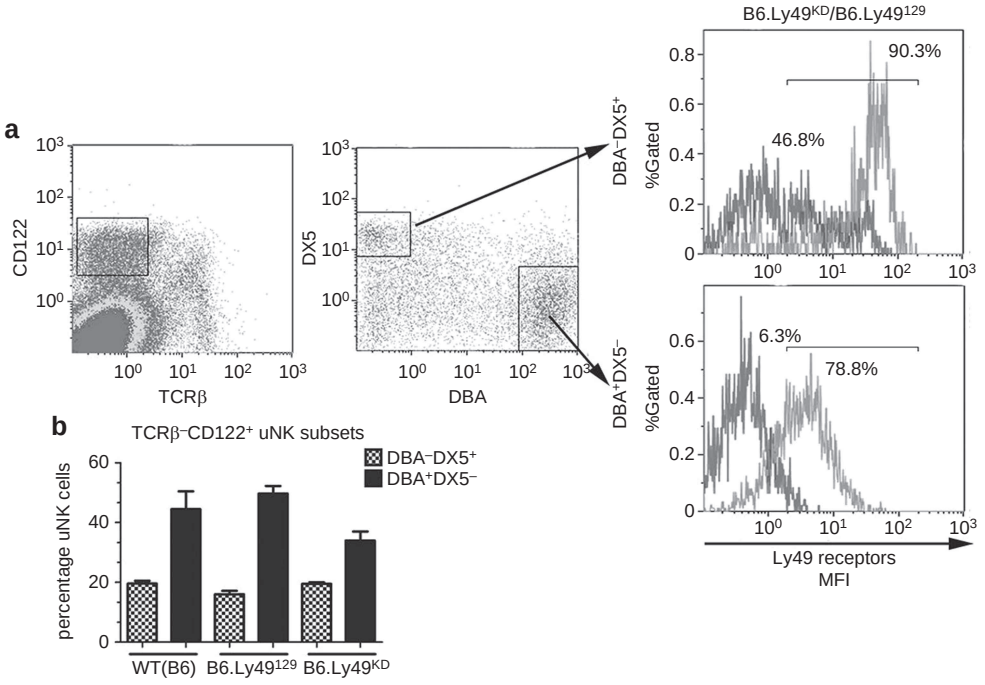

Figure 1 Ly49 receptor silencing in uNK cells from B6.Ly49^{KD} mice. Gd9.5 decidual cell flow cytometry of control, B6.Ly49^{129} and B6.Ly49^{KD} mice. (**a**) uNK cells were gated as TCRβ$^-$CD122$^+$ cells. From this gate, two uNK cells subsets were identified using DBA lectin and DX5 (anti-CD49B) binding. Both uNK cell subsets (DBA$^+$DX5$^-$; DBA$^-$DX5$^+$) express Ly49 receptors and the proportion of Ly49$^+$ cells was reduced in B6.Ly49^{KD} mice compared to controls. In B6.Ly49^{KD} mice, DX5$^+$DBA$^-$ cells were reduced ~50% (90.3%–47.8%); while DX5$^-$DBA$^+$ cells were reduced ~90% (78.8%–6.3%). The values represent an average of five independent experiments (five mice/genotype). (**b**) DBA$^+$DX5$^-$ and DBA$^-$DX5$^+$ uNK cells numbers were not significantly different among strains (*P>0.05). DBA$^+$DX5$^-$ and DBA$^-$DX5$^+$ uNK cells represented respectively in WT (B6) 48% and 20%; in B6.Ly49^{129} 51% and 17%; and in B6.Ly49^{KD} mice 34% and 20% of TCRβ$^-$CD122$^+$ cells. DBA, *Dolichos biflorus* agglutinin; gd, gestation day; KD, knockdown; uNK, uterine natural killer; WT, wild type.

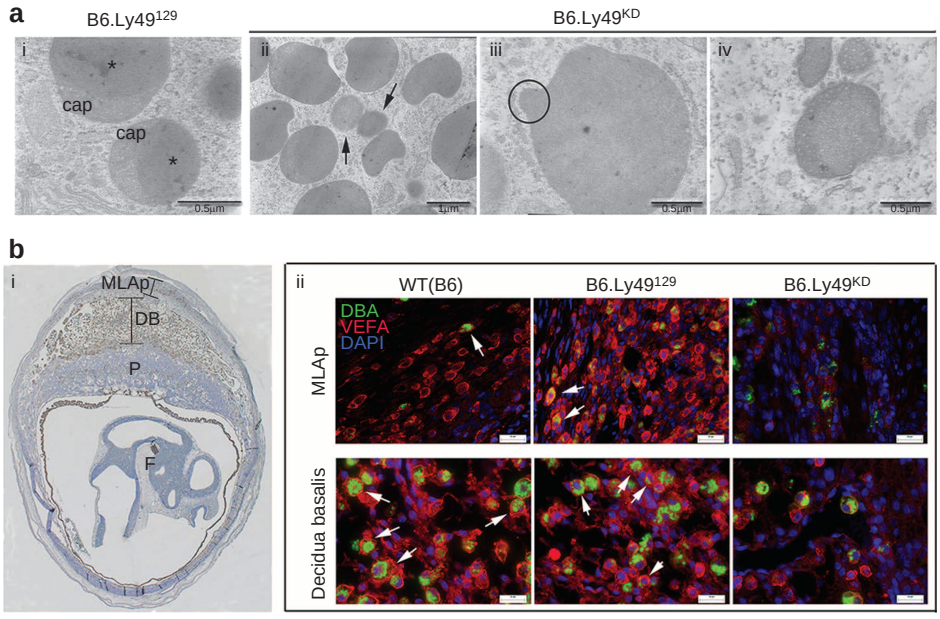

Figure 2 Granulogenesis and expression of VEGFA are impaired in B6.Ly49^{KD} uNK cells. (**a**) Ultrastructural features of normal uNK cell granules in gd10.5 B6.Ly49^{129} decidua are shown (**i**). The range of alterations detected in gd10.5 B6.Ly49^{KD} uNK cell granules is shown in **ii**–**iv**. (**ai**) The lysosomal-secretory granules from controls (B6.Ly49^{129}) as double-compartment organelles with lysosomal caps and solid secretory-cytotoxic (*) cores. Knockdown of Ly49 receptors altered granule structure (**aii**–**iv**). Smaller sizes (arrows), aberrant shapes (circle) and reduced multivesicular-bodies structures were common differences found in B6.Ly49^{KD} uNKs cell granules, suggesting a deficit in their biogenesis. (**bi**) is a photomicrograph representative of a gd10.5 implantation site labeled to identify specific mesometrial regions. (**bii**) depicts double immunocytochemistry using anti-VEGFA (Alexa-fluor594; red) and DBA lectin (FITC; green) at gd10.5. The top row illustrates representative images from the MLAp region of control (B6 and B6.Ly49^{129}) and B6.Ly49^{KD} mice. The bottom row illustrates the DB region in the same three strains. In both regions, uNK cells are coreactive to VEGFA and DBA lectin (arrows). VEGFA is reduced in DBA^{+}DX5^{-} uNK cells of B6.Ly49^{KD} mice, and in other non-identified decidual cells (n=3 pregnancies/genotype). Nuclei are identified by DAPI reactivity (blue). Bars: **ai**, **aiii**, **aiv**: 0.5 µm; **aii**): 1 µm; **b**: 20 µm. DB, decidua basalis; DBA, *Dolichos biflorus* agglutinin; F, fetus; gd, gestation day; KD, knockdown; MLAp: mesometrial lymphoid aggregate of pregnancy; P, placenta; uNK, uterine natural killer; VEGFA, vascular endothelial cell growth factor.

uNK cells are perforin^{+}; quantification of gd9.5 BALB/cJ perforin^{+} uNK cells found ~45% of DBA^{+} and ~7.5% of DBA^{-} uNK cells expressing perforin[21] (and unpublished data). At gd10.5, immunoreactivity of perforin in B6.Ly49^{KD} uNK cells did not differ from controls, despite the impaired granule biogenesis detected ultrastructurally. This suggests that the ultrastructural defects in B6.Ly49^{KD} uNK cells are more likely related to the formation of the lysosomal than the perforin-containing secretory compartment. Distribution of uNK cells expressing perforin between the MLAp and decidua basalis was similar in the three strains (Figure 3a).

IFNG concentrations in lysates of gd10.5 pooled MLAp and decidua basalis did not differ significantly among the strains (P>0.05; Figure 3b). These data suggest that IFNG, a product predominantly of DBA^{-} uNK cells,[24,34] is not affected by Ly49 receptor downregulation. Since reduced Ly49 receptor expression by uNK cells had the most dramatic impact on VEGFA production, further studies analysed decidual angiogenesis and spiral artery remodelling.

Impact of Ly49 KD on early decidual angiogenesis and implantation site growth

Whole-mount immunohistochemistry was used to analyse the potential impact of Ly49 KD on early (gd6.5) decidual angiogenesis. In controls, endothelial cells formed webs representative of intense angiogenesis and ~50% of the CD45^{+} cells in decidua basalis brightly co-expressed CD31, suggesting their activation (Figure 4a). In B6.Ly49^{KD} mice, angiogenesis had been initiated across the decidua and the decidua basalis contained approximately equal numbers of CD45^{+} cells of sizes, shapes and distributions resembling controls (Supplementary Figure 1). CD45^{+} cells however had reduced CD31 reactivity. Angiogenesis was present in B6.Ly49^{KD} decidua but it was less widespread (fewer angiogenic webs, intervessel linkages and more straight, distinct edge-defined vessels). Endothelial tip cell formation was more prominent in the basolateral decidua of control than B6.Ly49^{KD} decidua (Figures 4).

Implant site size was addressed in B6.Ly49^{KD} and control mice at gd9.5 and 10.5 (Supplementary Figures 2). At gd9.5, B6.Ly49^{KD} implant sites were statistically smaller (Supplementary Figure 2c). This appeared to be due to a smaller decidua basalis, a conclusion supported by immunohistochemistry for cytokeratin at gd10.5 (Figure 5a). This staining for trophoblast cell detection revealed no differences between the strains in the surface areas occupied by placental trophoblasts.

Impact of Ly49 receptor KD on spiral arterial remodelling

At gd10.5, morphometric analyses of spiral arteries revealed that the wall/lumen ratio was significantly higher in the

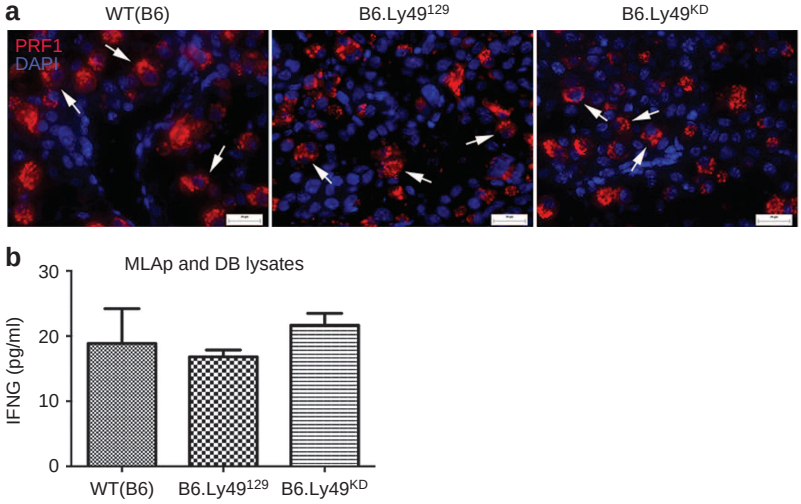

Figure 3 Perforin and IFNG expression are not altered in B6.Ly49^{KD} decidua at gd10.5. (**a**) Perforin (PRF1) expression was detected by immunocytochemistry (Alexa-fluor 594 anti-perforin/red) in uNK cells (arrows). No differences were apparent between the strains. (**b**) IFNG concentrations measured in the homogenate of litter-pooled, DB and MLAp are illustrated. IFNG concentrations were not significantly different between strains. Data were plotted as mean±s.e.m. (n=3 pregnancies/genotype and 2 experimental repetitions), B6 (18.86 pg/ml), B6.Ly49^{129} (16.82 pg/ml) and B6.Ly49^{KD} (21.65 pg/ml), with *P>0.05. Bars: **a**: 20 μm. DB, decidua basalis; gd, gestation day; KD, knockdown; MLAp: mesometrial lymphoid aggregate of pregnancy; uNK, uterine natural killer.

B6.Ly49^{KD} mice compared to B6.Ly49^{129} and B6 controls (Figure 5a and b; P<0.0001). To support the conclusion that spiral arterial remodelling was impaired, immunohistochemistry for actin^{+} vascular smooth muscle cells surrounding spiral arteries was conducted. More actin^{+} cells were present in the spiral arterial walls of B6.Ly49^{KD} than controls (Figure 5c).

Impact of Ly49 receptor KD on reproductive outcomes

A number of factors affect overall fertility. In our study, mating performance was assessed as the number of females with vaginal plugs but no evidence for implantation or post-implantation pregnancy loss compared to mated females with implantation sites on gd6.5, 9.5 or 10.5. Failure to establish pregnancy (i.e., a sterile mating with copulation detection) was common in B6.Ly49^{KD} mice (P<0.05) (Figure 6a). Absence of implantation sites could indicate female or male infertility, pre-implantation developmental delays or failure of either implantation or very early post-implantation events. Female B6.Ly49^{KD} showed normal estrous cycles, while male B6.Ly49^{KD} had histologically normal testes with seminiferous tubules of normal size and caliber containing spermatids (Figure 6B). Blastocysts isolated from the uterine lumen of B6.Ly49^{KD} on gd3.5 were at a morphologically normal, expanded but unhatched stage of development (Figure 6c). Thus, the effects of Ly49 KD on gametes and on pre-implantation development were excluded.

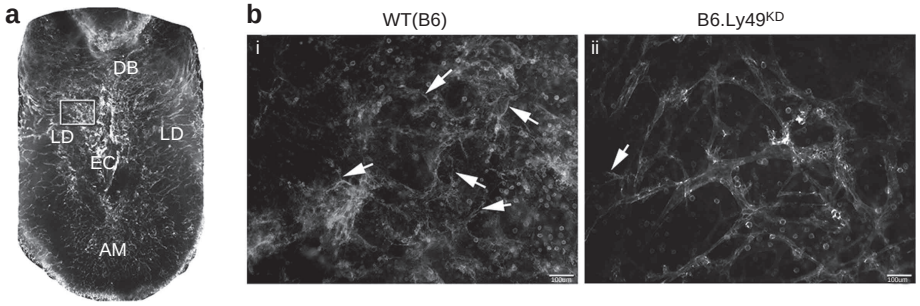

Figure 4 Downregulation of Ly49 receptors impairs early decidual angiogenesis. Whole mount *in situ* immunochemistry of viable, sagittally sectioned implantation sites using CD31 (PE; endothelial cell marker). (**a**) A control implantation site at gd6.5 shows the EC is surrounding by a super bright signal that first appears at gd6.5 (32). The arrangement and density of vessels differ between the AM, LD and DB. (**b**) Details of LD in control (**i**) and B6.Ly49^{KD} (**ii**) implantation sites are illustrated. Limited angiogenesis is observed in B6.Ly49^{KD} *versus* control mice as reduced brightness, predominance of black areas (tissue surrounding the vessels). Additionally, vascular straightness, less web formation, narrower vessels and fewer cellular projections (endothelial tip cells; arrows) were observed in B6.Ly49^{KD} mice. In addition to CD31^{+} vessel structures, round CD31^{+} leukocytes (identified as CD45^{+} cells—Supplementary Figure 1; Ref. 32) are observed in control mice. CD31 intensity was reduced in B6.Ly49^{KD} mice. The results are representative of two pregnant females/genotype. Bars=100 μm. AM, anti-mesometrial region; DB, decidua basalis; EC, embryonic crypt; gd, gestation day; KD, knockdown; LD, lateral deciduas.

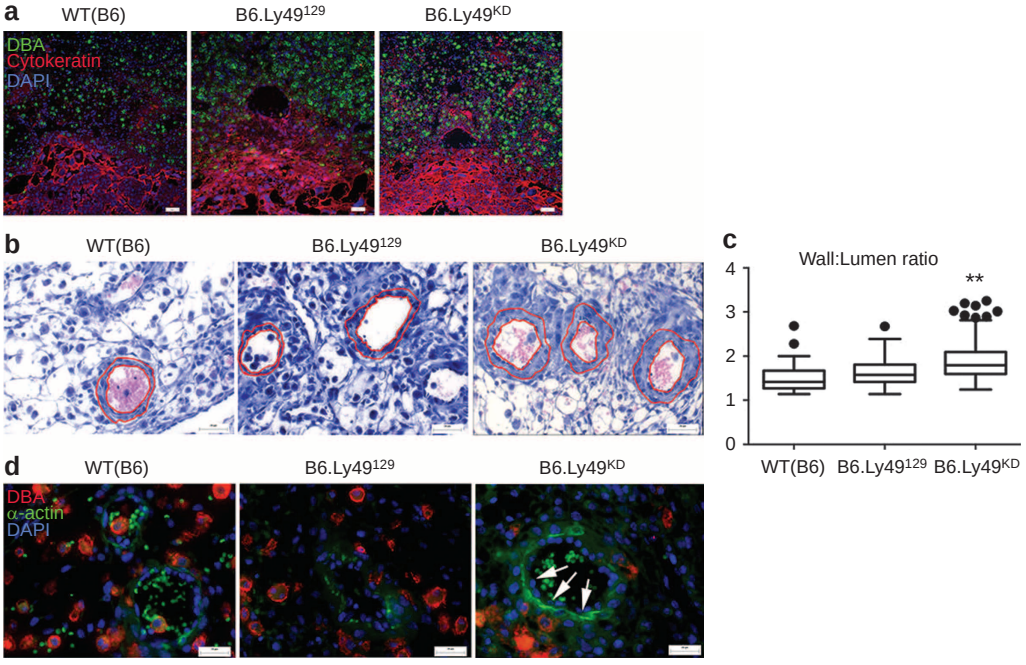

Figure 5 Downregulation of Ly49 receptors impairs spiral artery remodelling, but not trophoblast invasion at gd10.5. (**a**) Double staining using anti-cytokeratin (Alexa-fluor 594; red) and DBA lectin (FITC; green) showed that trophoblast invasion (cytokeratin$^+$ cells) was not impaired by Ly49 receptor knockdown. DAPI (blue) was used to identify nuclei. (**b**, **c**) Photomicrographs of H&E-stained gd10.5 implantation site sections showing the analytical approach for spiral artery morphometry. Spiral arterial wall/lumen ratios in B6.Ly49^{KD} were significantly greater than in control mice, indicating failure of remodelling. Data are plotted as mean±s.e.m. (3 pregnancies/genotype; 2 implantation sites/pregnancy; 3 slides/implantation site; 12 digital images/slide; $^{**}P \leqslant 0.01$). (**d**) Double staining using anti-alpha-actin (FITC; green) and DBA lectin (Texas red; red) is shown; alpha-actin is expressed by vascular smooth-muscle cells. In controls, spiral arterial walls had weak staining of discontinuous vascular smooth-muscle cells. Spiral arteries of B6.Ly49^{KD} decidua had strong staining of actin that was continuous around most of vessel wall. Bars: **a**: 100 μm; **b**, **d**: 20 μm. DBA, *Dolichos biflorus* agglutinin; gd, gestation day; KD, knockdown.

These data collectively suggest that implantation/peri-implantation failures account for the subfertility (high number of sterile matings) in B6.Ly49^{KD} mice.

The interval between copulation and delivery of pups was measured and its mean value did not differ between strains (range for 10 litters/genotype was 19–21 days). Although gestation length and mean litter sizes were similar between genotypes (Figure 6d), B6.Ly49^{KD} neonates were heavier than B6.Ly49^{129} neonates at birth (Figure 6e), indicating macrosomia. This may reflect intrauterine or maternal cardiovascular compensatory responses to the impaired early decidual angiogenesis and spiral arterial remodelling seen in B6.Ly49^{KD} pregnancies.

DISCUSSION

UNK cells are well-characterized lymphocytes of early human and mouse decidua. In both species, uNK cells are functionally heterogeneous. In mice, two major subsets are defined by reactivity to DBA lectin.[24] Here, we report that expression of Ly49 receptors differs between these two subsets. In normal control mice, both DBA$^+$DX5$^-$ and DBA$^-$DX5$^+$ uNK cells express Ly49 receptors (78.8% and 90.3%, respectively). Genetic KD of Ly49 had a greater impact on DBA$^+$DX5$^-$ uNK cells (>10-fold reduction from 78.8% to 6.3%) than on DBA$^-$DX5$^+$uNK cells (approximately halved from 90.3% to 46.8%). The former uNK cells are a unique angiogenic subset found in decidua, while the latter resemble splenic NK cells and are distinguishable by their production of IFNG.[24] Ly49 receptor KD significantly decreased VEGFA production, early decidual angiogenesis and mid-pregnancy spiral arterial remodelling, but had no detectable effect on decidual levels of IFNG or on uNK cell production of perforin.

Numbers of uNK cells present in MLAp and decidua basalis of B6.Ly49^{KD} mice were unaltered by reduced Ly49 receptor expression. However, the terminal maturation or activation of the cells appeared to be altered because the cytoplasm of most B6.Ly49^{KD} uNK cells contained mixtures of normal and abnormal granules or only abnormal granules (Figure 2a). Some uNK cells contained only well-formed cytoplasmic granules that, by ultrastructure, were equivalent to those in control uNK cells. We postulate that these represent the small proportions of DBA$^+$ and DBA$^-$uNK cells that lacked detectable Ly49 by flow cytometry (Figure 1). This is the first demonstration that Ly49 receptors influence NK cell granule biogenesis. We demonstrate that Ly49 receptors are involved in angiogenic factor induction in DBA$^+$DX5$^-$ uNK cells. This conclusion is consistent with RNA analyses that identified the DBA$^+$ uNK cell subset as more angiogenic than DBA$^-$ uNK cells.[24] Reduced decidual VEGFA production is also consistent with the reduced early decidual angiogenesis observed in B6.Ly49^{KD}

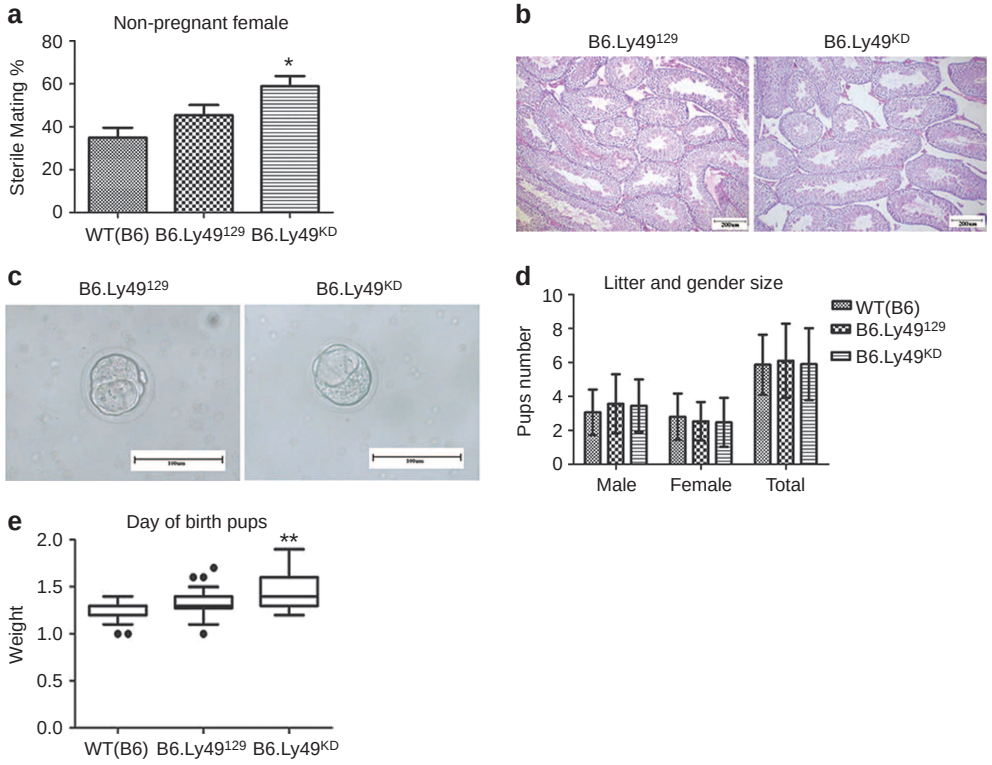

Figure 6 Reproductive outcomes in B6.Ly49^{KD} mice. (**a**) Percentage of sterile matings scored as the number of non-pregnant mice following detection of a vaginal copulation plug with absence of resorbing implantation sites at gd6.5–10.5. Values are plotted as percentage (mean±s.e.m.; n=103 (WT (B6)); n=106 (B6.Ly49^{129}); n=104 (B6.Ly49^{KD}); *$P\leqslant0.05$). (**b**) Testis morphology between B6.Ly49^{129} and B6.Ly49^{KD} mice did not differ (n=2 males/genotype). Seminiferous tubules were normal in size and caliber and contained spermatids in all strains. (**c**) Expanded blastocysts were flushed in equal numbers from gd3.5 B6.Ly49^{129} and B6.Ly49^{KD} mice. (**d**) Litter sizes were evaluated by pup sex and number. These did not differ between strains. (**e**) At birth, B6.Ly49^{KD} pups were significantly heavier (1.455 g; **$P\leqslant0.01$) than B6 (1.265 g) or B6.Ly49^{129} (1.332 g) pups. The high incidence of sterile matings in B6.Ly49^{KD} mice was attributed to pre- or peri-implantation embryo loss. Bars: **b**: 200 μm; **c**: 100 μm. gd, gestation day; KD, knockdown; WT, wild type.

decidua by whole mount study (Figure 4). A reported observation that gd5.5 CD3$^-$CD122$^+$NK1.1$^+$ uNK cells (i.e., DBA$^-$ subset) do not produce VEGFA after 4 h of culture with anti-Ly49D antibody is consistent with our conclusion that DBA-uNK cells are not an angiogenesis-promoting cell population.[35]

IFNG concentrations in decidua basalis were unaffected by Ly49 receptor KD. This outcome coincides with earlier studies that show IFNG synthesis by B6.Ly49^{KD} splenic NK cells is normal after stimulation with target cells (RMA-S or YAC-1), crosslinked anti-natural cytotoxicity triggering receptor 1, pharmacological induction or murine CMV infection.[30] These data indicate that IFNG expression is not Ly49 receptor-dependent, but is dependent upon NKG2D,[36] a functional receptor in B6.Ly49^{KD} mice.[30] Since some studies suggest that uNK cells use a different transcription factor for IFNG regulation than peripheral NK cells,[37] alternative explanations for normal levels of IFNG in B6.Ly49^{KD} decidua basalis must also be considered. For example, DBA$^-$DX5$^+$ uNK cells that are responsible for most to all of the IFNG production in early decidua were much less severely affected by the Ly49 KD than the angiogenic DBA$^+$ uNK cells. Thus, residually expressed Ly49 receptors may provide sufficient signaling for normal levels of IFNG production. IFNG is reported to be the key molecule regulating initiation of mouse spiral arterial remodelling.[34,38] However, despite normal IFNG concentrations in B6.Ly49^{KD} decidua, spiral arterial remodelling was impaired. Multiple mechanisms contribute to the structural changes of spiral arteries including extracellular matrix restructuring, endothelial and smooth muscle cell de-differentiation, migration and proliferation, changes in cell adhesion and sensitivity to death-inducing stimuli.[10,39,40] The positioning and localized delivery of IFNG by uNK cells in support of any of these processes may be inappropriate or insufficient in B6.Ly49^{KD} to effect remodelling. Alternatively, other cell types may be compensating sources of IFNG in B6.Ly49^{KD}, and not properly localized to be effective in driving this remodelling. Our observation of residual smooth muscle surrounding B6.Ly49^{KD} spiral arteries may implicate a VEGFA deficit, since VEGFA affects vascular smooth muscle cell changes *via* endothelial cell modulated vasodilation,[41] pericyte regulation[42] and expression of actin.[43]

The Ly49 receptor family appears to regulate the typical gd5.5–6.5 transition in many CD45$^+$ cells from CD31$^-$ to CD31$^+$ detected by whole mount staining. In other studies, the strongly reactive CD45$^+$CD31$^+$ decidual cells were shown to be uNK cells.[14] While the role of CD31-expressing lymphocytes are best defined in T cells, it is postulated that activated

NK cells use homotypic CD31 interactions to lyse $CD4^+$ T cells, B cells and dendritic cells.[44] The Ly49 receptor family is not the only receptor pathway involved in uNK cell activation. Two other receptors activated by non-MHC ligands, aryl hydrocarbon receptor and natural cytotoxicity triggering receptor 1 (the human NKp46 homologue), independently activate uNK cells. Similar to B6.Ly49^{KD} and uNK cell-deficient mice, mice with genetic inactivation of *Ahr* or *Ncr1* lack spiral arterial modification and have developmentally delayed embryos prior to opening of the placental circulation (gd9.5–10).[45] In a preliminary study, we measured gd9.5 B6.Ly49^{KD} implantation sites and found that they were smaller than controls (Supplementary Figure 2). Thus, a series of mouse models that lack uNK cells or uNK cell activation now align with human genetic data to support the importance of uNK cells and of their activation in establishing the early intrauterine conditions for developmentally appropriate conceptus growth. Subfertility was also identified in B6.Ly49^{KD} mice. Since developmentally normal blastocysts were present at gd3.5, hatching or uterine attachment of blastocysts must have been impaired. This was not an anticipated outcome because it occurs before uNK cell differentiation. This finding may indicate an importance for fertility promotion in mice by Ly49-expressing cell types rather than uNK cells or an importance of circulating NK cells. In the fertility-compromising KIRAA/HLA-C combinations in humans, infertility is also seen.[5] Whether murine studies attributing subfertility to loss after expanded blastocyst development is translational to humans must be considered cautiously since menstrual cycle and pregnancy-induced uNK cells are already present in human decidua before blastocyst hatching.

If pregnancy was established in B6.Ly49^{KD} mice, it appeared to proceed normally with duration and litter sizes matching controls, despite deviations in decidual vascular remodelling. Compensatory mechanisms appeared to maintain B6.Ly49^{KD} pregnancies and shift conceptuses from growth restricted prior to placental function to overgrown by term. In other mouse models with impaired decidual vascular remodelling, ultrasonography identified anomalous gains in cardiac stroke volume and output with left ventricular dilation as compensatory processes during pregnancy.[46] In contrast to human studies,[5] evidence for spontaneous abortion was not present in B6.Ly49^{KD} mice. It is possible that genes other than Ly49 contribute to the reproductive alterations seen in B6.Ly49^{KD} mice. The generation of this strain[30] involved gain of DNA from a *Klra15* (Ly49O) targeting construct sequence, which integrated as a concatemer in the NKC. This insertion leads not only to regional transcriptional silencing and loss of most Ly49 receptor expression, but also to slight downregulation of transcription of neighboring genes encoding the CD94/NKG2 and KLRI receptors. Some of these receptors, such as NKG2D, have roles in the pregnancy.[47] However, because B6.Ly49^{KD} mice have reduced cytotoxicity against target cells expressing MHC-I ($B2m^{-/-}$, $H2K^{-/-}$ or $H2D^{-/-}$ cells) and normal cytotoxicity against NKG2D ligand-positive cells (YAC-1 and RMA-S-Rae-1), it is probable that the pregnancy-associated alterations observed in B6.Ly49^{KD} mice are due solely to the Ly49 deficiency.

In sum, the significant findings of this study are that failure of uNK cells to engage Ly49 receptors impacts uNK cell subsets differently, with greater impact upon the angiogenic subset that is unique to decidua. It impedes cytoplasmic granule biogenesis in a selective manner that impairs the lysosomal compartment, but spares $perforin^+$ granule cores and it dramatically reduces uNK cell VEGFA, uNK cell-promoted early decidual angiogenesis and spiral arterial remodelling. These insights may assist in defining the mechanisms underlying the protective effects of KIR activation in human pregnancy.

CONFLICT OF INTEREST

The authors declare no conflicts of interest.

ACKNOWLEDGEMENTS

This study was funded by the Canadian Institutes of Health Research (CIHR; MOP 62841 to APM and MOP 77519 to BAC) and NSERC (RGPIN3219 to BAC). MMT is supported by an Ontario Graduate Scholarship.

Supplementary Information accompanies the paper on *Cellular & Molecular Immunology*'s website (http://www.nature.com/cmi).

1 Peel S, Granulated metrial gland cells. *Adv Anat Embryol Cell Biol* 1989; **115**: 1–112.
2 Bulmer JN, Morrison L, Longfellow M, Ritson A, Pace D. Granulated lymphocytes in human endometrium: histochemical and immunohistochemical studies. *Hum Reprod* 1991; **6**: 791–798
3 Gellersen B, Brosens IA, Brosens JJ. Decidualization of the human endometrium: mechanisms, functions, and clinical perspectives. *Semin Reprod* 2007; **25**: 445–453.
4 Weir PE, Oats JN, Holdsworth R, Cross R. Histocompatibility antigens and intrauterine fetal growth retardation. *Aust NZ J Obstetr Gynaecol* 1985; **25**: 108–110.
5 Hiby SE, Apps R, Sharkey AM, Farrell LM, Gardner L, Mulder A *et al*. Maternal activating KIRs protect against human reproductive failure mediated by fetal HLA-C2. *J Clin Inv* 2010; **120**: 4102–4110.
6 Christiansen OB. Reproductive immunology. *Mol Immunol* 2013; **55**: 8–15.
7 Hiby SE, Walker JJ, O'Shaughnessy KM, Redman CW, Carrington M, Trowsdale J *et al*. Combinations of maternal KIR and fetal HLA-C genes influence the risk of preeclampsia and reproductive success. *J Exp Med* 2004; **200**: 957–965.
8 Parham P, Norman PJ, Abi-Rached L, Hilton HG, Guethlein LA. Review: immunogenetics of human placentation. *Placenta* 2012; **33**(Suppl): 71–80.
9 Xiong S, Sharkey AM, Kennedy PR, Gardner L, Farrell LE, Chazara O *et al*. Maternal uterine NK cell-activating receptor KIR2DS1 enhances placentation. *J Clin Invest* 2013; **123**: 28–30.
10 Bulmer JN, Innes BA, Levey J, Robson SC, Lash GE. The role of vascular smooth muscle cell apoptosis and migration during uterine spiral artery remodeling in normal human pregnancy. *FASEB J* 2012; **26**: 2975–2985.
11 Li C, Houser BL, Nicotra ML, Strominger JL. HLA-G homodimer-induced cytokine secretion through HLA-G receptors on human decidual macrophages and natural killer cells. *Proc Natl Acad Sci USA* 2009; **106**: 5767–72.
12 Hanna J, Goldman-Wohl D, Hamani Y, Avraham I, Greenfield C, Natanson-Yaron S *et al*. Decidual NK cells regulate key

developmental processes at human fetal–maternal interface. *Nat Med* 2006; **12**: 1065–1074.
13 Ashkar AA, Di Santo JP, Croy BA. Interferon gamma contributes to initiation of uterine vascular modification, decidual integrity, and uterine natural killer cell maturation during normal murine pregnancy. *J Exp Med* 2000; **192**: 259–270.
14 Hofmann AP, Gerber SA, Croy BA. Uterine natural killer cells pace early development of mouse decidua basalis. *Mol Hum Reprod* 2013; **20**: 66–76.
15 Tayade C, Hilchie D, He H, Fang Y, Moons L, Carmeliet P *et al*. Genetic deletion of placenta growth factor in mice alters uterine NK cells. *J. Immunol* 2007; **178**: 4267–4275.
16 Zhang JH, Yamada AT, Croy BA. DBA-lectin reactivity defines natural killer cells that have homed to mouse decidua. *Placenta* 2009; **30**: 968–973.
17 Paffaro JrVA, Bizinotto MC, Joazeiro PP, Yamada AT. Subset classification of mouse uterine natural killer cells by DBA lectin reactivity. *Placenta* 2003; **24**: 479–488.
18 Madeja Z, Yadi H, Apps R, Boulenouar S, Roper SJ, Gardner L. Paternal MHC expression on mouse trophoblast affects uterine vascularization and fetal growth. *Proc Natl Acad Sci USA* 2011; **108**: 4012–4017.
19 Parr EL, Young LH, Parr MB, Young JD. Granulated metrial gland cells of pregnant mouse uterus are natural killer-like cells that contain perforin and serine esterases. *J Immunol* 1990; **145**: 2365–2369.
20 Zheng LM, Joag SV, Parr MB, Parr EL, Young JD. Perforin-expressing granulated metrial gland cells in murine deciduoma. *J Exp Med* 1991; **174**: 1221–1226.
21 Lima PDA, Croy BA, Degaki KY, Tayade C, Yamada AT. Heterogeneity in composition of mouse uterine natural killer cell granules. *J Leuk Biol* 2012; **92**: 195–204.
22 Croy BA, Zhang J, Tayade C, Colucci F, Yadi H, Yamada AT. Analysis of uterine natural killer cells in mice. In: Campbell KS (ed.) *Natural Killer Cell Protocols*. Totowa, NJ: Humana Press, 2010: 465–503.
23 Yadi H, Burke S, Madeja Z, Hemberger M, Moffett A, Colucci F. Unique receptor repertoire in mouse uterine NK cells. *J Immunol* 2008; **181**: 6140–6147.
24 Chen Z, Zhang J, Hatta K, Lima PD, Yadi H, Colucci F *et al*. DBA-lectin reactivity defines mouse uterine natural killer cell subsets with biased gene expression. *Biol Reprod* 2012; **87**: 81.
25 De SF, Segura I, de BK, Hohensinner PJ, Carmeliet P. Mechanisms of vessel branching: filopodia on endothelial tip cells lead the way. *Arter Thromb Vas Biol* 2009; **29**: 639–649.
26 Degaki KY, Chen Z, Yamada AT, Croy BA. Delta-like ligand (DLL)1 expression in early mouse decidua and its localization to uterine Natural Killer cells. *PLoS ONE* 2012; **7**: e52037.
27 Kume T. Novel insights into the differential functions of Notch ligands in vascular formation. *J Angiogenes Res* 2009; **1**: 8.
28 Yokoyama WM, Plougastel BF. Immune functions encoded by the natural killer gene complex. *Nat Rev Immunol* 2003; **3**: 304–316.
29 Carlyle JR, Mesci A, Fine JH, Chen P, Bélanger S, Tai LH *et al*. Evolution of the Ly49 and Nkrp1 recognition systems. *Semin Immunol* 2008; **20**: 321–330.
30 Bélanger S, Tu MM, Rahim MM, Mahmoud AB, Patel R, Tai LH *et al*. Impaired natural killer cell self-education and ''missing-self'' responses in Ly49-deficient mice. *Blood* 2012; **120**: 592–602.
31 Patel R, Bélanger S, Tai LH, Troke AD, Makrigiannis AP. Effect of Ly49 haplotype variance on NK cell function and education. *J Immunol* 2010; **185**: 4783–4792.
32 Croy BA, Chen Z, Hofmann AP, Lord EM, Sedlacek AL, Gerber SA. Imaging of vascular development in early mouse decidua and its association with leukocytes and trophoblasts. *Biol Reprod* 2012; **87**: 125.
33 Nagy A, Gertsenstein M, Vintersten K, Beheringer R. Collecting blastocyst. In: *Manipulating the Mouse Embryo: A Laboratory Manual*. 3rd ed. New York: Cold Spring Harbor Laboratory Press, 2003: 201–203.
34 Ashkar AA, Croy BA. Interferon-γ contributes to the normalcy of murine pregnancy. *Biol Reprod* 1999; **61**: 493–502.
35 Chiossone L, Vacca P, Orecchia P, Croxatto D, Damonte P, Astigiano S *et al*. *In vivo* generation of decidual natural killer cells from resident hematopoietic progenitors. *Haematologica* 2013; **99**: 448–457.
36 Carayannopoulos LN, Barks JL, Yokoyama WM, Riley JK. Murine trophoblast cells induce NK cell interferon-gamma production through KLRK1. *Biol Reprod* 2010; **83**: 404–414.
37 Tayade C, Fang Y, Black GP Jr, Paffaro VA, Erlebacher A, Croy BA. Differential transcription of Eomes and T-bet during maturation of mouse uterine natural killer cells. *J Leuk Biol* 2005; **78**: 1347–1355.
38 Monk JM, Leonard S, McBey BA, Croy BA. Induction of murine spiral artery modification by recombinant human interferon-gamma. *Placenta* 2005; **26**: 835–838.
39 Whitley GS, Cartwright JE. Cellular and molecular regulation of spiral artery remodeling: lessons from the cardiovascular field. *Placenta* 2010; **31**: 465–474.
40 Nanaev A, Chwalisz K, Frank HG, Kohnen G, Hegele-Hartung C, Kaufmann P. Physiological dilation of uteroplacental arteries in the guinea pig depends on nitric oxide synthase activity of extravillous trophoblast. *Cell Tissue Res* 1995; **282**: 407–421.
41 Prisby R, Menezes T, Campbell J. Vasodilation to PTH (1–84) in bone arteries is dependent upon the vascular endothelium and is mediated partially *via* VEGF signaling. *Bone* 2013; **54**: 68–75.
42 Greenberg JI, Shields DJ, Barillas SG, Acevedo LM, Huang J, Scheppke L *et al*. A role for VEGF as negative regulator of pericyte function and vessel maturation. *Nature* 2009; **456**: 809–813.
43 Butler SM, Abrassart JM, Hubbell MC, Adeoye O, Semotiuk A, Williams JM *et al*. Contributions of VEGF to age-dependent transmural gradients in contractile protein expression in ovine carotid arteries. *Am J Physiol Cell Physiol* 2011; **301**: 653–666.
44 Marelli-Berg FM, Clement M, Mauro C, Caligiuri G. An immunologist's guide to CD31 function in T-cells. *J Cell Sci* 2013; **126**: 2343–2352.
45 Felker AM, Chen Z, Foster WG, Croy BA. Receptors for non-MHC ligands contribute to uterine natural killer cell activation during pregnancy in mice. *Placenta* 2013; **1**: 4–11.
46 Zhang J, Adamns MA, Croy BA. Alterations in maternal and fetal heart functions accompany failed spiral arterial remodeling in pregnant mice. *Am J Obstet Gynecol* 2011; **205**: 485.e1–485.e16.
47 Thaxton JE, Nevers T, Lippe EO, Blois SM, Saito S, Sharma S. NKG2D blockade inhibits poly(I:C)-triggered fetal loss in wild type but not in IL-10$^{-/-}$ mice. *J Immunol* 2013; **190**: 3639–3647.